

Physical-Parameter Identification of Base-Isolated Buildings Using Backbone Curves

Ming-Chih Huang¹; Yen-Po Wang²; Jer-Rong Chang³; and Yi-Hsuan Chen⁴

Abstract: In this paper, a simplified system identification procedure is developed to investigate the dynamic characteristics of base-isolated buildings equipped with lead-rubber bearings (LRBs). The multistory superstructure is assumed to be linear on the account of substantial reduction in seismic forces due to the installation of LRBs for which a bilinear hysteretic model is considered. The hysteretic model is in turn characterized by a backbone curve by which the multivalued restoring force is transformed into a single-valued function. With the introduction of backbone curves, the system identification analysis of inelastic structures is simplified to a large extent. The proposed algorithm extracts individually the physical parameters of each floor and the bearing system that are considered useful information in the structural health monitoring. A numerical example is conducted to demonstrate the feasibility of using the proposed technique for physical-parameter identification of partially inelastic based-isolated buildings.

DOI: 10.1061/(ASCE)ST.1943-541X.0000047

CE Database subject headings: Base isolation; Parameters; Identification; Hysteresis; Curvature; Inelasticity.

Introduction

Seismic base isolation is an effective means of damage-proof of building structures against strong earthquakes. The idea of base isolation is to lengthen the fundamental period of the structures so as to avoid resonance with the predominant frequency contents of the earthquakes. Thus, the seismic responses of a base-isolated building can be significantly reduced in comparison with its non-isolated counterpart. Various base isolation systems have been extensively studied both analytically and experimentally since the early 1970's (Kelly 1986; Koh and Kelly 1989; Fan and Ahmadi 1992; Pan and Cui 1994; Chung et al. 1999; Hwang and Hsu 2000; Jangid and Kelly 2001) and they have been widely adopted all over the world nowadays. Among others, the lead-rubber bearing (LRB) has been the most popular base-isolation system adopted for practical implementation in New Zealand, Japan, the United States, Italy, China, and Taiwan (Shinner et al. 1993; Li and Wu 2006; Lee et al. 2003). Recently, the base-isolation technique has been considered even for earthquake protection of tall buildings such as the 32-story Los Angeles city halls, 18-story Oakland city hall, and numerous other projects in Japan (Keri and

Anil 2006; Pan et al. 2005). Over the last decade, design guidelines and codes with the ordinances of base-isolated buildings have been developed for engineering practice. They include the Uniform Building Code, International Building Code, and China Design Code for Aseismic Buildings (ICBO 1997; ICC 1998; CDCAB 2000).

It is not attainable to artificially test massive civil engineering structures for the realization of their dynamic behaviors. Seismic structural responses recorded during earthquake episodes, instead, provide useful information at modest costs in gaining insight into the behavior and characteristics of the structures via the application of system identification techniques. System identification is an inverse problem of structural dynamics that is adopted for the estimation of structural parameters based on the measured responses of structures and input disturbances. System identification techniques classified as the output-error methods (Maia and Silva 1997; Chaudhary et al. 2000) commonly refer to those that determine the system parameters by minimizing the discrepancies between the measured responses and the estimates of the structure or model. The identification methods can be categorized into time-domain and frequency-domain approaches. In a frequency-domain approach, modal quantities such as the natural frequencies, damping ratios, and mode shapes are commonly identified from the frequency response functions. In a time-domain method, the system parameters, such as the stiffness and damping coefficient or modal quantities, can be determined with the data in time series. The identification methods, on the other hand, can also be categorized into modal-parameter identification and physical-parameter identification approaches. The former commonly refers to those identifying the invariable dynamic properties of structural systems without presuming a physical model while the latter refers to those obtaining system parameters in relation to a desired or expected physical model. The physical-parameter identification approach is important for reliability enhancement in the design of active structural control systems or realization of seismic performance of base-isolated structures. The development of such system identification schemes is quite limited, however, because they require data acquisition of nearly full-state responses

¹Assistant Professor, Dept. of Aircraft Engineering, Air Force Institute of Technology, Gangshan, 820 Taiwan, Republic of China; mailing address: Jyulun Rd., Gangshan Township, Kaoshiung County, 820 Taiwan, Republic of China (corresponding author). E-mail: sander.huang@msa.hinet.net

²Professor, Dept. of Civil Engineering, National Chiao Tung Univ., Hsinchu, 300 Taiwan, Republic of China.

³Associate Professor, Dept. of Aircraft Engineering, Air Force Institute of Technology, Gangshan, 820 Taiwan, Republic of China.

⁴Graduate Student, Dept. of Civil Engineering, National Chiao Tung Univ., Hsinchu, 300 Taiwan, Republic of China.

Note. This manuscript was submitted on June 10, 2008; approved on February 27, 2009; published online on March 26, 2009. Discussion period open until February 1, 2010; separate discussions must be submitted for individual papers. This paper is part of the *Journal of Structural Engineering*, Vol. 135, No. 9, September 1, 2009. ©ASCE, ISSN 0733-9445/2009/9-1107-1114/\$25.00.

of the structure and entangled manipulations, in particular, for inelastic systems. A mixed approach in which the physical parameters are identified from the modal parameters of the system predetermined by a modal-parameter system identification approach has also been proposed (Loh et al. 2000; Housner et al. 1997; Takewaki and Nakamura 2005).

The construction of base-isolated structures has rapidly increased after the invasion of mass destructive earthquake events in the United States (1994 Northridge), Japan (1995 Kobe) and Taiwan (1999 Ji-Ji) in recent years. In spite of limited number of recorded seismic response data, vigorous studies to appraise the actual behavior of base-isolated structures during strong earthquakes have been conducted. Nagarajaiah and Sun (2000) studied the response of a base-isolated hospital building in the University of Southern California (USC) using the recorded seismic response data of the 1994 Northridge earthquake. The study indicated that the identified responses using a bilinear model for the base-isolation system showed good agreement with the observed data and the superstructure was found elastic due to the effectiveness of base isolation. Chaudhary et al. (2000) proposed a two-step system identification method for identifying the structural parameters from strong motion records. The physical parameters of the structures were estimated using a modal model. This study showed that the proposed method was capable of capturing the overall behavior of the base-isolated structures with an effective equivalent stiffness and two-degree-of-freedom (2DOF) lumped mass models. Nagarajaiah and Sun (2001) explored the seismic performance of the base isolated building of fire command and control (FCC). A two-dimensional (2D) analytical model with the impact-spring-dashpot was proposed to reflect the dynamic properties of the structural system under impact loading. A three-dimensional (3D) analytical model that accounted for the effects of eccentric impact loading with respect to the center of mass was further developed to estimate the lateral-torsional response of the base-isolated building. The simulation results based on the identified parameters and the proposed analytical model were quite accurate in comparison with the recorded data. The study indicated that the seismic performance of the FCC building in the Northridge earthquake was satisfactory, except that the shear forces and drift were increased due to the impulsive waves in the ground excitation. Furukawa et al. (2005) proposed a prediction error method with a nonlinear state-space model using the Gauss-Newton iterative procedure for the identification of a base-isolated structure with bidirectional seismic response data. Several inelastic restoring force-displacement models have been considered to represent the base-isolation system, including the bilinear model, bilinear multiple shear spring (MSS) model, and trilinear MSS model. Results indicated that the trilinear hysteretic MSS model best fitted the actual hysteretic restoring force profile and time histories observed. Nagarajaiah and Dharap (2003) developed a new approach for system identification of base-isolated buildings. A least-squares technique with time segments was proposed for the identification of piecewise linear systems. A series of equivalent linear system parameters were identified from segment to segment. A reduced-order observer was used in the lack of full-state measurements to estimate the unmeasured states and initial conditions at each time segment. The evolving equivalent linear dynamic properties of the USC hospital building during the Northridge earthquake were identified using the proposed technique. The change of system parameters, such as the frequencies and damping ratios, due to inelastic behavior of the LRBs were reliably estimated. Nagarajaiah and Li (2004) conducted the system identification of the FCC building by using the same tech-

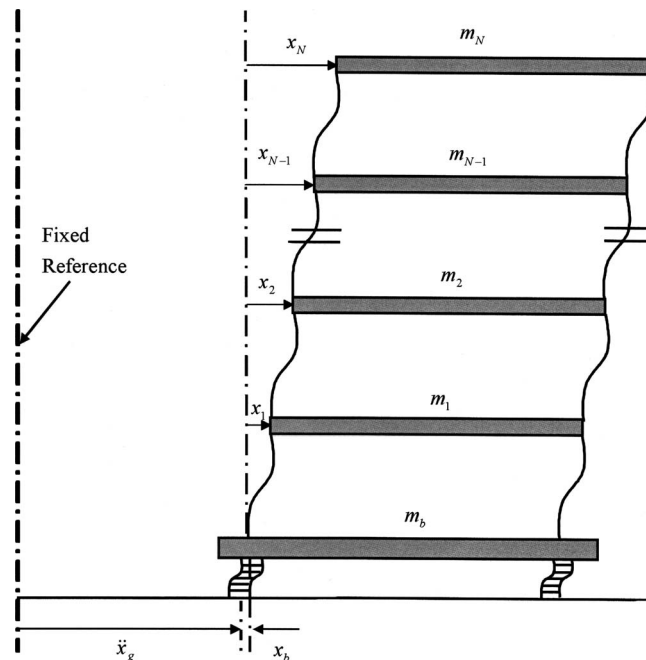


Fig. 1. Isolated building

nique. Yoshimoto et al. (2005) proposed a damage detection algorithm for the structural monitoring of base-isolated buildings. The modal participation factors were taken into account to identify the input-output relations for each mode under a multiinput and multioutput frameworks. Three types of simplified models, including the rigid equivalent linear single-story and uniform multistory model were considered to comply with the partial-state observation of the structural responses as it was commonly the case in practice. Results indicated that the uniform multistory model gave the most precise prediction of seismic responses, despite the actual interstory stiffness and damping coefficients of the target structure were not identified.

In this paper, a simplified system identification process is developed to investigate the dynamic characteristics of base-isolated buildings equipped with LRBs. The superstructure of multistories is assumed to be linear but not necessarily uniformly distributed on the account of substantial reduction in seismic forces due to the installation of LRBs for which a bilinear hysteretic model is considered. The hysteretic model is, in turn, characterized by a backbone curve by which the multivalued restoring force is transformed into a single-valued function. With the introduction of backbone curves, the system identification analysis of inelastic structures is simplified to a large extent. The proposed algorithm extracts individually the physical parameters of each floor and the bearing system that are considered useful information in the structural health monitoring. A numerical example is conducted to demonstrate the feasibility of using the proposed technique for the physical-parameter identification of partially inelastic base-isolated buildings.

Motion Equation

Consider a linear N -story shear type structure mounted on a base-isolated foundation with LRBs, as shown in Fig. 1. The LRBs are installed between the base and foundation. This measure aims to reduce the seismic forces in the superstructure. The reduction in

When Eq. (10) is substituted by Eq. (4), the governing equation of the base at instant i becomes

$$m_b \ddot{x}_b^i + c_b \dot{x}_b^i + h_b(x_b^i) + 2f_b \left(\frac{x_b^i - x_b^l}{2} \right) - C_1 \dot{x}_1^i - K_1 x_1^i = -m_b \ddot{x}_g^i \quad (12)$$

At instant $i=I$, the above equation reduces to

$$h_b(x_b^I) = -m_b \ddot{x}_b^I - c_b \dot{x}_b^I + C_1 \dot{x}_1^I + K_1 x_1^I - m_b \ddot{x}_g^I \quad (13)$$

Substituting Eq. (13) for $h_b(x_b^I)$ into Eq. (12), one gets

$$m_b(\ddot{x}_b^i - \ddot{x}_b^I) + c_b(\dot{x}_b^i - \dot{x}_b^I) + 2f_b \left(\frac{x_b^i - x_b^I}{2} \right) = -m_b(\ddot{x}_g^i - \ddot{x}_g^I) + C_1(\dot{x}_1^i - \dot{x}_1^I) + K_1(x_1^i - x_1^I) \quad (14)$$

Defining

$$u_b^i = x_b^i - x_b^I \quad (15)$$

in Eq. (11) and substituting it into Eq. (14), the governing equation can be rewritten as

$$\ddot{u}_b^i + \frac{c_b}{m_b} \dot{u}_b^i + \frac{k_{eb}}{m_b} u_b^i = \ddot{u}_g^i - D \leq u_b^i/2 \leq D \quad (16)$$

$$\ddot{u}_b^i + \frac{c_b}{m_b} \dot{u}_b^i + \frac{2b_b}{m_b} + \frac{k_{yb}}{m_b} u_b^i = \ddot{u}_g^i u_b^i/2 > D \quad (17)$$

$$\ddot{u}_b^i + \frac{c_b}{m_b} \dot{u}_b^i - \frac{2b_b}{m_b} + \frac{k_{yb}}{m_b} u_b^i = \ddot{u}_g^i - u_b^i/2 < -D \quad (18)$$

where

$$\ddot{u}_g^i = -(\ddot{x}_g^i - \ddot{x}_g^I) + \frac{C_1}{m_b}(\dot{x}_1^i - \dot{x}_1^I) + \frac{K_1}{m_b}(x_1^i - x_1^I) \quad (19)$$

Eqs. (16)–(18) are used to identify the parameters of the bearings.

Identification Processes

Identification of the system parameters can be conducted once the dynamic responses of the structure subjected to the input excitation are available. Based on an output-error concept (Maia and Silva 1997; Chaudhary et al. 2000), the system parameters are obtained by minimizing the discrepancy between the recorded and predicted responses of the system. The system parameters so evaluated are considered optimal.

All the available dynamic response data are classified into three groups based on the state of displacement depicted in Eq. (11). The process of identification starts by assuming an arbitrary initial value of C_1 in Eq. (19). An optimal K_1 is obtained via an iterative procedure until the criterion of convergence is achieved. Then, K_1 is fixed at this value and the process proceeded toward the determination of an optimal C_1 . Meanwhile, the corresponding system parameters c_b , b_b , k_{eb} , and k_{yb} are alternately yielded.

Using the first set of data for $|u_b^i/2| \leq D$ and Eq. (16), we define the partial measure of fit as

$$e_1 = \sum_{i=1} \left[\ddot{u}_b^i + \frac{c_b}{m_b} \dot{u}_b^i + \frac{k_{eb}}{m_b} u_b^i - \ddot{u}_g^i \right]^2 \quad (20)$$

The values of c_b and k_{eb} are obtained by simultaneously solving

$$\frac{\partial e_1}{\partial(c_b/m_b)} = 0 \quad \frac{\partial e_1}{\partial(k_{eb}/m_b)} = 0 \quad (21)$$

Similarly, application of the second data set for $u_b^i/2 > D$ and Eq. (17) produces another partial measure of fit as

$$e_2 = \sum_{i=1} \left[\ddot{u}_b^i + \frac{c_b}{m_b} \dot{u}_b^i + \frac{2b_b}{m_b} + \frac{k_{yb}}{m_b} u_b^i - \ddot{u}_g^i \right]^2 \quad (22)$$

extremization of Eq. (22) with respect to the unknowns yields

$$\frac{\partial e_2}{\partial(c_b/m_b)} = 0 \quad \frac{\partial e_2}{\partial(2b_b/m_b)} = 0 \quad \frac{\partial e_2}{\partial(k_{yb}/m_b)} = 0 \quad (23)$$

from which the values of c_b , b_b , and k_{yb} are obtained. Finally, application of the third data set for $-u_b^i/2 < -D$ and Eq. (18), the third partial measure of fit is defined as

$$e_3 = \sum_{i=1} \left[\ddot{u}_b^i + \frac{c_b}{m_b} \dot{u}_b^i - \frac{2b_b}{m_b} + \frac{k_{yb}}{m_b} u_b^i - \ddot{u}_g^i \right]^2 \quad (24)$$

The minimization of e_3 with respect to c_b/m_b , $2b_b/m_b$, and k_{yb}/m_b leads to

$$\frac{\partial e_3}{\partial(c_b/m_b)} = 0 \quad \frac{\partial e_3}{\partial(2b_b/m_b)} = 0 \quad \frac{\partial e_3}{\partial(k_{yb}/m_b)} = 0 \quad (25)$$

The parameters c_b , b_b , and k_{yb} are obtained by solving Eq. (25) simultaneously. The global measure of fit is defined as the sum of all partial ones as

$$e = e_1 + e_2 + e_3 \quad (26)$$

The set of c_b , b_b , k_{eb} , k_{yb} , c_1 , and K_1 that gives the minimum global measure of fit is regarded as the solution. Moreover, the parameters identified from the data of multiple hysteresis loops are somewhat different from cycle to cycle. This is attributed to the amplitude-dependent nature of the hysteretic behavior that cannot be fully traced by the simplified bilinear model. In such a circumstance, the average value of all is adopted.

The equation for identifying the damping coefficient and stiffness of the second floor by using Eq. (3) is derived as

$$\ddot{x}_1 - \frac{C_2}{m_1}(\dot{x}_2 - \dot{x}_1) - \frac{K_2}{m_1}(x_2 - x_1) = -(\ddot{x}_g + \ddot{x}_b) - \frac{C_1}{m_1} \dot{x}_1 - \frac{K_1}{m_1} x_1 \quad (27)$$

An error function for the Floor 2 is defined as

$$e_{f2} = \sum_{i=1} \left[\ddot{x}_1 + \frac{C_1}{m_1} \dot{x}_1 + \frac{K_1}{m_1} x_1 - \frac{C_2}{m_1}(\dot{x}_2 - \dot{x}_1) - \frac{K_2}{m_1}(x_2 - x_1) - \ddot{x}_g + \ddot{x}_b \right]^2 \quad (28)$$

in which the updated values of C_1 and K_1 are adopted. The values of C_2 and K_2 are then obtained by simultaneously solving

$$\frac{\partial e_{f2}}{\partial(C_2/m_1)} = 0 \quad \frac{\partial e_{f2}}{\partial(K_2/m_1)} = 0 \quad (29)$$

By the same token, the equation for identifying the system parameters of the j th floor by Eq. (2) is expressed as

$$\ddot{x}_{j-1} - \frac{C_j}{m_{j-1}}(\dot{x}_j - \dot{x}_{j-1}) - \frac{K_j}{m_{j-1}}(x_j - x_{j-1}) = -(\ddot{x}_g + \ddot{x}_b) - \frac{C_{j-1}}{m_{j-1}}(\dot{x}_{j-1} - \dot{x}_{j-2}) - \frac{K_{j-1}}{m_{j-1}}(x_{j-1} - x_{j-2}) \quad (30)$$

and the error function for the j th floor is defined as

$$e_{jj} = \sum_{i=1} \left[\ddot{x}_{j-1} + \frac{C_{j-1}}{m_{j-1}}(\dot{x}_{j-1} - \dot{x}_{j-2}) + \frac{K_{j-1}}{m_{j-1}}(x_{j-1} - x_{j-2}) - \frac{C_j}{m_{j-1}}(\dot{x}_j - \dot{x}_{j-1}) - \frac{K_j}{m_{j-1}}(x_j - x_{j-1}) + \ddot{x}_g + \ddot{x}_b \right]^2 \quad (31)$$

extremization of Eq. (31) with respect to the unknowns yields

$$\frac{\partial e_{jj}}{\partial(C_j m_{j-1})} = 0 \quad \frac{\partial e_{jj}}{\partial(K_j m_{j-1})} = 0 \quad (32)$$

With C_{j-1} and K_{j-1} derived already from the previous step, C_j and K_j are obtained by solving Eq. (32) simultaneously for $j=3 \sim N$. This constitutes one complete cycle of the identification process once all the system parameters are identified. The procedure of the identification process is summarized below as:

Step 1. Assume the yielding displacement D of the LRB. In the j -th iterative loop, $D^j = D^{j-1} + dD$, where $dD = \max|u_b^1|/100$, $D^0 = 0$, and $j=100$ are considered.

Step 2. Assume K_1 and C_1 for Eq. (19), where, for the k -th iteration, $K_1^k = K_1^{k-1} + dK$ with $dK = 10$ MN/m.

Step 3. Solve for c_b , b_b , k_{eb} , and k_{yb} by Eq. (21), Eq. (23), or Eq. (25) based on the yielding displacement D assumed in Step 1 and calculate the global measure of fit e by Eq. (26). Repeat Steps 2–3 for $k=1 \sim 100$. The most possible set of parameters K_1 , c_b , b_b , k_{eb} , and k_{yb} corresponds to the minimum e for all k .

Step 4. Assume K_1 and C_1 for Eq. (19) with K_1 determined from Step 3 and $C_1^l = C_1^{l-1} + dC$ with $dC = 50$ kN s/m.

Step 5. Solve for c_b , b_b , k_{eb} , and k_{yb} by Eq. (21), Eq. (23), or Eq. (25) based on the yielding displacement D assumed in Step 1 and calculate the global measure of fit, e , by Eq. (26). Repeat Steps 4–5 for $l=1 \sim 50$. The most possible set of parameters C_1 , c_b , b_b , k_{eb} , and k_{yb} corresponds to the minimum e for all l .

Step 6. Repeat Steps 1–5 for $j=1 \sim 100$. The most possible set of parameters K_1 , C_1 , c_b , b_b , k_{eb} , and k_{yb} corresponds to the minimum e for all l .

Step 7. Determine C_j and K_j of the j -th floor for $j=2 \sim N$ by minimizing Eq. (28) or Eq. (31) with the previously determined K_{j-1} and C_{j-1} .

This completes one cycle of the iterative process. The accuracy of the identification may be further refined with the updated yielding displacement $D \approx b_b / (k_{eb} - k_{yb})$ of the LRB and a smaller increment of the stiffness and damping coefficient for K_1 and C_1 , say $dK = 1$ MN/m and $dC = 1$ kN s/m for the second cycle, $dK = 1$ MN/m and $dC = 1$ kN s/m for the third cycle, etc.

Moreover, to assess the overall accuracy of the identification process, an error index (EI) is defined as

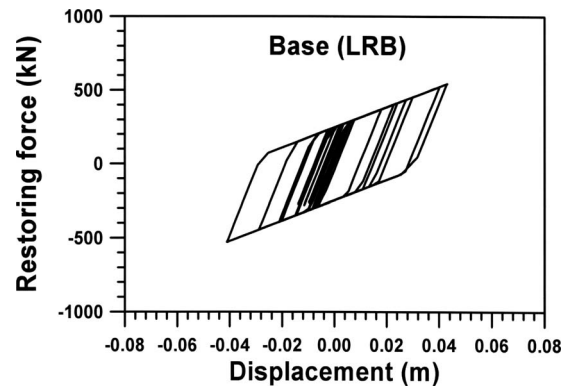


Fig. 3. Nonlinear restoring force of LRB

$$EI = \left\{ \frac{\int_0^t [(\ddot{x}_j)_r - (\ddot{x}_j)_i]^2 dt}{\int_0^t [(\ddot{x}_j)_r]^2 dt} \right\}^{1/2} \quad (33)$$

where $(\ddot{x}_j)_r$ = recorded or measured acceleration response of the j -th floor and $(\ddot{x}_j)_i$ = corresponding theoretical or predicted response. The latter is calculated from the identified system parameters with the recorded input excitation. When j is replaced by b , Eq. (33) represents the EI for the base.

Numerical Example

As an effort to verify the proposed methodology for system identification of based-isolated buildings, a numerical example is considered using a three-story shear building with a plane of 9×9 m² and story height of 3 m. The isolation layer consists of five LRB bearings. The system parameters considered in this study include: (1) $m_1 = m_2 = m_3 = 58.32 \times 10^3$ kg, $k_1 = 256.15$ MN/m, $k_2 = 168.06$ MN/m, and $k_3 = 104.92$ MN/m for the superstructure; and (2) $m_b = 68.04 \times 10^3$ kg, $b_b = 245.25$ kN, $k_{eb} = 44.145$ MN/m, and $k_{yb} = 6.867$ MN/m for the base and LRB. Moreover, the damping ratios of the superstructure and LRB are assumed to be 0.05 and 0.07, respectively. The damping coefficients are converted to be $C_1 = 494$ kN s/m, $C_2 = 324$ kN s/m, $C_3 = 202$ kN s/m, and $c_b = 156$ kN s/m based on the concept of composite modal damping and Rayleigh damping (Pu 1995; Hwang and Chiou 1996; Clough and Penzin 1993).

The fundamental period of the structure is increased from 0.298 to 1.964 s with the installation of LRBs. The dynamic responses of the superstructure and base under the N -S component of the 1940 El Centro earthquake are calculated using Newmark's linear acceleration method with a time-step of 0.02 s. The acceleration responses contaminated with an artificial white noise signal of 5% noise-to-signal ratio are considered in the system identification analysis to simulate the measured data in a more realistic manner.

Fig. 3 presents the nonlinear restoring force of LRB with a yielding displacement of 0.658 cm and a ductility ratio of 7.322. The force-displacement relationship of the story shear at the first floor is almost linear, as illustrated in Fig. 4.

In the first cycle of the identification process, the initial value of C_1 is arbitrarily set to be zero. The global measure of fit with respect to K_1 is presented in Fig. 5 from which the least-squares

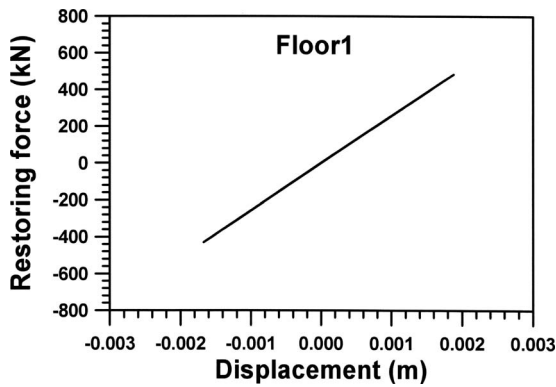


Fig. 4. Restoring force and displacement of Floor 1

estimate of K_1 is shown to be 250.0 MN/m. The minimization process is then proceeded further to find C_1 and other system parameters by keeping K_1 at this value. The optimal estimate of C_1 reads 440 kN s/m, as illustrated in Fig. 6. Meanwhile, the parametric values of LRB are identified as $c_b=155$ kN s/m, $b_b=240.96$ kN, $k_{eb}=43.554$ MN/m and $k_{yb}=6.766$ MN/m. Then, substituting $C_1=440$ kN s/m and $K_1=250.0$ MN/m into Eq. (28) and carrying out the minimization process, the parametric values of Floor 2 are identified in succession as $C_2=273$ kN s/m and $K_2=164.86$ MN/m. Finally, the optimal estimate of C_3 and K_3 of the third floor are obtained in a similar

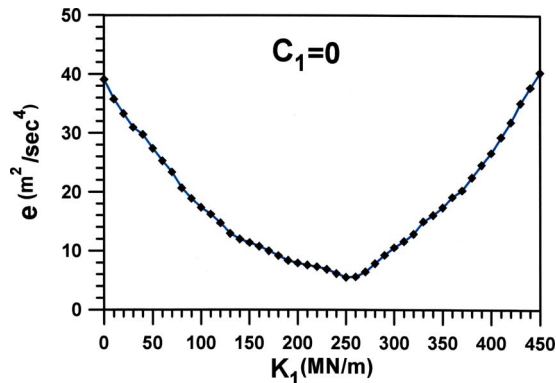


Fig. 5. Global measure of fit in the first cycle setting $C_1=0$ kN s/m

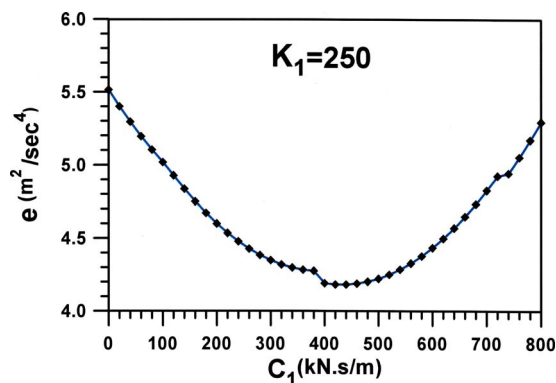


Fig. 6. Global measure of fit in the first cycle setting $K_1=250$ MN/m

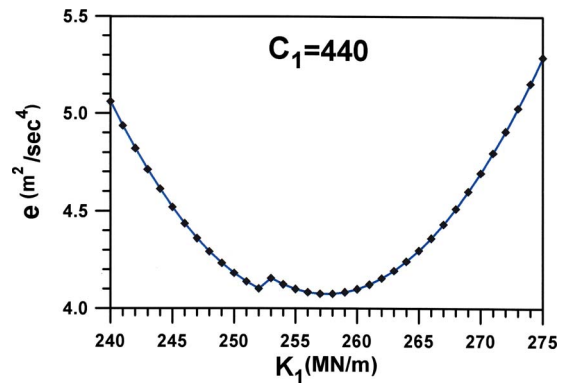


Fig. 7. Global measure of fit in the second cycle setting $C_1=440$ kN s/m

manner by Eq. (31) as $C_3=162$ kN s/m and $K_3=102.67$ MN/m, respectively. This constitutes one cycle of the identification.

The second iterative cycle is next proceeded by considering the initial value of C_1 as 440 kN s/m derived from the previous cycle. Minimizing the global measure of fit, we have $K_1=258.0$ MN/m, as shown in Fig. 7. Table 1 summarizes the system parameters of the LRB and the first floor identified, respectively, in three iterative cycles while Table 2 summarizes the parameters of Floor 2 and Floor 3. Numerical results in this example suggest that three iterative cycles of identification are enough for sufficient accuracy. In addition, the skeleton curve (backbone curve) estimated from the identified parameters of LRB using the Masing criterion is illustrated in Fig. 8. The comparisons of the base acceleration and displacement are shown, respectively, in Figs. 9 and 10 and the third floor acceleration and displacement responses, respectively, in Figs. 11 and 12. Good agreement between the identified and measured responses has been observed, indicating adequacy of the proposed identification scheme for partially inelastic dynamic systems.

Conclusions

This paper develops a procedure for identification of the structural parameters of base-isolated buildings equipped with LRBs. The nonlinear behavior of the LRB is, for simplicity, characterized with a bilinear skeleton curve by which the multivalued restoring force of displacement is transformed into a single-valued function to minimize the computational effort in the identification analysis. Feasibility of the proposed scheme has been demonstrated via a numerical example of a based-isolated multistory structure subjected to earthquake ground excitations. The features of the proposed procedure include the following:

- The physical parameters of a partially inelastic multidegree-of-freedom (MDOF) system can be extracted directly. This method can be extended for system identification of the building structures implemented with energy-dissipative seismic dampers if they can be represented with some form of skeleton curves.
- All interstory structural parameters, such as the stiffness and damping coefficients, can be individually identified. This method is not restricted to uniform buildings with identical structural parameters in all stories and considered a potential tool for damage assessment and health monitoring of structural systems.

Table 1. Identified Parameters of LRB and Floor 1

Number of cycle	c_b (kN s/m)	b_b (kN)	k_{yb} (MN/m)	k_{eb} (MN/m)	C_1 (kN s/m)	K_1 (MN/m)
1	155	240.96	6.766	43.554	440	250.00
2	156	247.17	6.890	44.490	433	258.00
3	156	246.74	6.880	44.409	430	257.40
True value	156	245.25	6.867	44.145	494	256.15
EI		0.3757			0.3581	

Table 2. Identified Parameters of Floors 2 and 3

Number of cycle	C_2 (kN s/m)	K_2 (MN/m)	C_3 (kN s/m)	K_3 (MN/m)
1	273	164.86	162	102.67
2	288	169.55	187	106.23
3	285	168.96	178	105.71
True value	324	168.06	202	104.92
EI	0.3419		0.3957	

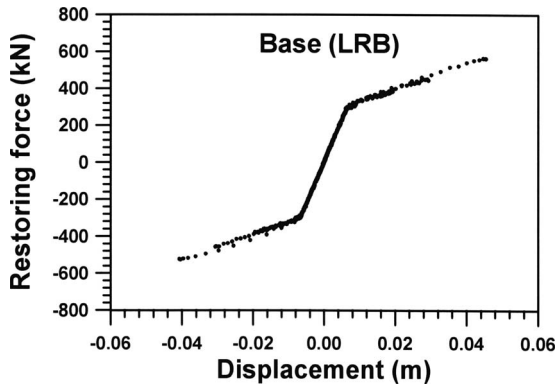


Fig. 8. Identified skeleton curve of LRB

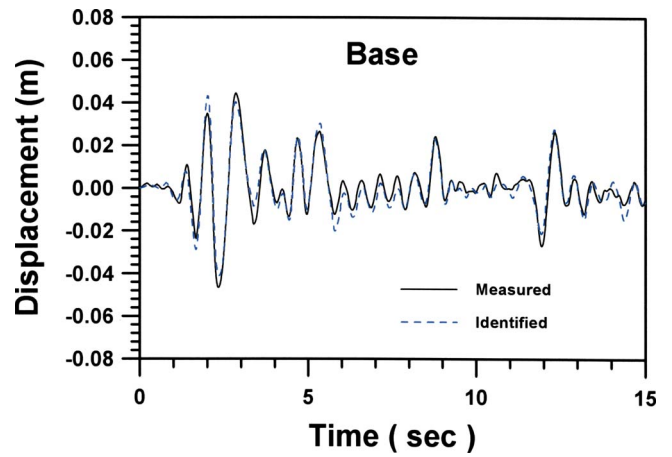


Fig. 10. Comparison between identified and measured displacements of base

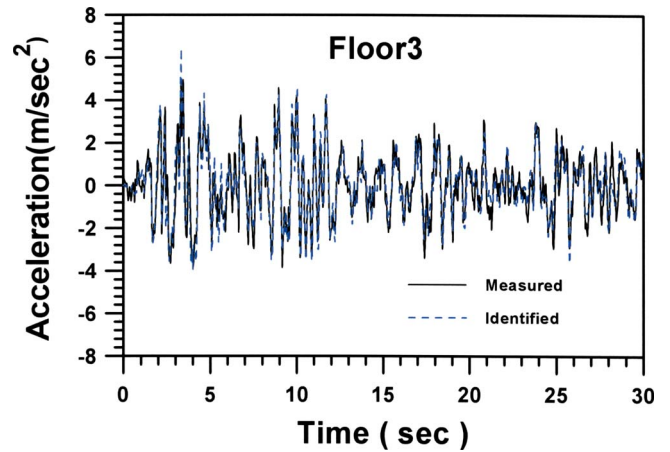


Fig. 11. Comparison between identified and measured accelerations of Floor 3

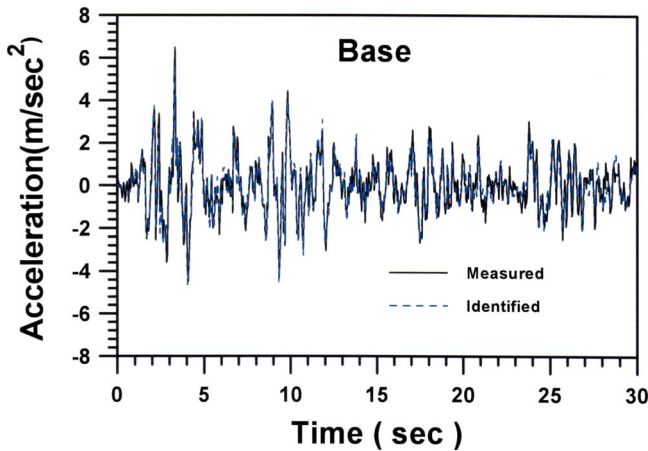


Fig. 9. Comparison between identified and measured accelerations of base

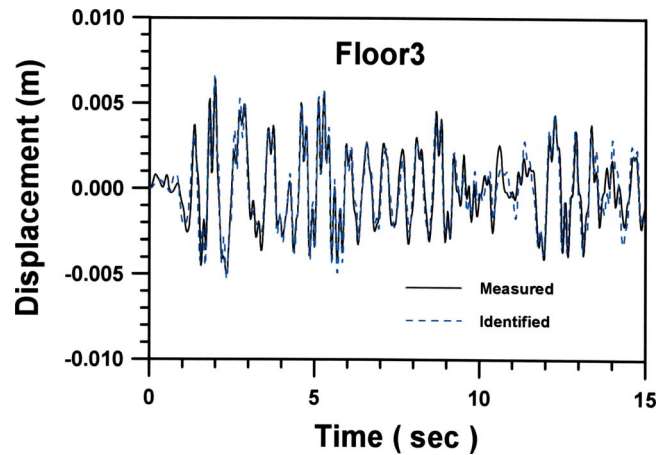


Fig. 12. Comparison between identified and measured displacements of Floor 3

- The system parameters are identified with reasonable accuracy in three iterations even in the presence of a 5% noise contamination. The robustness of the algorithm makes it favorable for practical applications.
- It is noted that, by the proposed method, the measurement of ground acceleration and full-state response data including acceleration, velocity, and displacement of all degrees of freedom is required. As in most occasions, only the acceleration responses are measured. In this case, the responses of the velocity and displacement need to be integrated from the acceleration records with baseline correction. This may inevitably introduce error to the physical parameters identified.

Acknowledgments

This work is partially supported by the National Science Council of the Republic of China (Contract No. NSC96-2625-Z-344-001).

References

- Chaudhary, M. T. A., Abe, M., Fujino, Y., and Yoshida, J. (2000). "System identification of two base-isolated bridges using seismic records." *J. Struct. Eng.*, 126(10), 1187–1195.
- China design code for aseismic buildings (CDCAB). (2000). China Standard and Code Committee, China Building Industrial Press, Beijing.
- Chung, W. J., Yun, C. B., Kim, N. S., and Seo, J. W. (1999). "Shaking table and pseudodynamic tests for the evaluation of the seismic performance of base-isolated structures." *Eng. Struct.*, 21(4), 365–379.
- Clough, R. W., and Penzlin, J. (1993). *Dynamics of structures*, 2nd Ed., McGraw-Hill, New York.
- Fan, F. G., and Ahmadi, G. (1992). "Seismic responses of secondary systems in base-isolated structures." *Eng. Struct.*, 14(1), 35–48.
- Furukawa, T., Ito, M., Izawa, K., and Noori, M. N. (2005). "System identification of base-isolated building using seismic response data." *J. Eng. Mech.*, 131(3), 268–275.
- Housner, G., Bergman, L. A., and Caughey, T. K. (1997). "Structural control: Past, present, and future." *J. Eng. Mech.*, 123(9), 897–971.
- Huang, M. C., and Tan, Y. R. (2003). "System identification of isolated bridge with consideration of bridge-soil interaction." *The Chinese Institute of Civil and Hydraulic Engineering*, 15(4), 773–788.
- Hwang, W. J., and Hsu, T. Y. (2000). "Experimental study of isolated building under triaxial ground excitations." *J. Struct. Eng.*, 126(8), 879–886.
- Hwang, J. S., and Chiou, J. M. (1996). "An equivalent linear model of lead-rubber seismic isolation bearings." *Eng. Struct.*, 18(7), 528–536.
- International Code Council (ICC). (1998). *International building code*, Whittier, Calif.
- International Conference of Building Officials (ICBO). (1997). *Uniform building code*, Whittier, Calif.
- Iwan, W. D. (1967). "On a class of models for the yielding behavior of continuous and composite system." *J. Appl. Mech.*, 34, 612–617.
- Jangid, R. S., and Kelly, J. M. (2001). "Base isolation for near fault motions." *Earthquake Eng. Struct. Dyn.*, 30(5), 691–707.
- Jennings, P. C. (1965). "Earthquake response of yielding structure." *J. Engrg. Mech. Div.*, 91, 41–68.
- Kelly, J. M. (1986). "A seismic base isolation: Review and bibliography." *Soil Dyn. Earthquake Eng.*, 5(4), 202–217.
- Keri, L. R., and Anil, K. C. (2006). "Estimating seismic demands for isolation bearings with building overturning effects." *J. Struct. Eng.*, 123(7), 1118–1128.
- Koh, C. G., and Kelly, J. M. (1989). "Viscoelastic stability model for elastomeric isolation bearings." *J. Struct. Eng.*, 115(2), 285–302.
- Lee, Z. K., Wu, T. H., and Lo, C. H. (2003). "System identification on the seismic behavior of an isolated bridge." *Earthquake Eng. Struct. Dyn.*, 32, 1797–1812.
- Li, H. N., and Wu, X. X. (2006). "Limitations of height-to-width ratio for base-isolated buildings under earthquake." *Struct. Des. Tall Spec. Build.*, 15, 277–287.
- Loh, C. H., Lin, C. Y., and Huang, C. C. (2000). "Time domain identification of frames under earthquake loadings." *J. Eng. Mech.*, 126(7), 693–707.
- Maia, N. M. M., and Silva, J. M. M., eds. (1997). *Theoretical and experimental modal analyses*, Research Studies Press Ltd., Taunton, U.K.
- Nagarajaiah, S., and Dharap, P. (2003). "Reduced order observer based identification of base isolated buildings." *Earthquake Eng. Eng. Vib.*, 2(2), 237–244.
- Nagarajaiah, S., and Li, Z. (2004). "Time segmented least squares identification of base isolated buildings." *Soil Dyn. Earthquake Eng.*, 24, 577–586.
- Nagarajaiah, S., and Sun, X. (2000). "Response of base-isolated USC hospital building in Northridge earthquake." *J. Struct. Eng.*, 126(10), 1177–1186.
- Nagarajaiah, S., and Sun, X. (2001). "Base-isolated FCC building: Impact response in Northridge earthquake." *J. Struct. Eng.*, 127(9), 1063–1075.
- Pan, P., Zambirescu, D., Nakayasu, M., and Kashiwa, H. (2005). "Base-isolation design practice in Japan: Introduction to the post-Kobe approach." *J. Earthquake Eng.*, 9(1), 147–171.
- Pan, T. C., and Cui, W. (1994). "Dynamic characteristics of shear buildings on laminated rubber bearings." *Earthquake Eng. Struct. Dyn.*, 23(12), 1315–1329.
- Pu, J. P. (1995). "Soil-structure interaction of base-isolated bridges" *Rep. No. NSC84-2211-E-035-003*, National Science Council, Taiwan, R.O.C.
- Shinner, R. I., Robinson, W. H., and McVerry, G. H. (1993). *An introduction to seismic isolation*, Wiley, New York.
- Takewaki, I., and Nakamura, M. (2005). "Stiffness-damping simultaneous identification under limited observation." *J. Eng. Mech.*, 131(10), 1027–1035.
- Yoshimoto, R., Mita, A., and Okada, K. (2005). "Damage detection of base-isolated buildings using multiinput multioutput subspace identification." *Earthquake Eng. Struct. Dyn.*, 34, 307–324.